

Hidden Critical Points in the Two-Dimensional $O(n > 2)$ Model: Exact Numerical Study of a Complex Conformal Field Theory


Arijit Haldar^{1,2,*}, Omid Tavakol^{4,1,*}, Han Ma,³ and Thomas Scaffidi^{4,1}

¹Department of Physics, University of Toronto, 60 Saint George Street, Toronto, Ontario M5S 1A7, Canada

²S. N. Bose National Centre for Basic Sciences, JD Block, Sector-III, Salt Lake City, Kolkata—700 106, India

³Perimeter Institute for Theoretical Physics, Waterloo, Ontario N2L 2Y5, Canada

⁴Department of Physics and Astronomy, University of California, Irvine, California 92697, USA

 (Received 10 April 2023; revised 26 August 2023; accepted 29 August 2023; published 27 September 2023)

The presence of nearby conformal field theories (CFTs) hidden in the complex plane of the tuning parameter was recently proposed as an elegant explanation for the ubiquity of “weakly first-order” transitions in condensed matter and high-energy systems. In this work, we perform an exact microscopic study of such a complex CFT (CCFT) in the two-dimensional $O(n)$ loop model. The well-known absence of symmetry-breaking of the $O(n > 2)$ model is understood as arising from the displacement of the nontrivial fixed points into the complex temperature plane. Thanks to a numerical finite-size study of the transfer matrix, we confirm the presence of a CCFT in the complex plane and extract the real and imaginary parts of the central charge and scaling dimensions. By comparing those with the analytic continuation of predictions from Coulomb gas techniques, we determine the range of validity of the analytic continuation to extend up to $n_g \approx 12.34$, beyond which the CCFT gives way to a gapped state. Finally, we propose a beta function which reproduces the main features of the phase diagram and which suggests an interpretation of the CCFT as a liquid-gas critical point at the end of a first-order transition line.

DOI: [10.1103/PhysRevLett.131.131601](https://doi.org/10.1103/PhysRevLett.131.131601)

Introduction.—The notion of universality at continuous phase transitions is central to our understanding of most phases of matter. However, there are several examples of “weakly first-order” transitions in high-energy and condensed matter physics which appear continuous at intermediate scales but eventually turn out to be first-order at larger scales [1–15]. One example is 4D gauge theories coupled to matter for which the gauge coupling is conjectured to run slowly (“walking behavior”) at intermediate energies but starts running fast again at low energies, leading to confinement and chiral symmetry breaking (“conformality loss”) [6]. Another example is the 2D classical Q -state Potts model, for which the ferromagnetic phase transition is second-order for $Q \leq 4$, but becomes weakly first order for Q slightly above 4 [1,2,10,13]. Further, numerical studies of the transition between Neel and valence bond solid states also point toward a weakly first-order scenario [7,8,12,15].

Recently, it was proposed that fixed point annihilation [7,8], and more specifically the resulting presence of complex conformal field theories (CCFTs) [9,10] hidden in the complex plane of the tuning parameter, could explain the widespread occurrence of weakly first-order transitions. In this scenario, the slow RG flow on the real axis is explained by the presence of a nearby CCFT in the complex plane, and the properties of the approximately conformal theory observed at intermediate scales can be derived from the complex conformal data of the CCFT. Complex

conformal field theories (CFTs) are nonunitary CFTs with highly unusual behavior, since they have complex central charge and scaling dimensions, and the RG flow around them forms a spiral. Exploring complex CFTs is also relevant from the perspective of understanding phase transitions in dissipative quantum systems described by non-Hermitian Hamiltonians [16–27].

The study of CCFTs is however challenging, and few models and results exist [9,10,13,14,28–32]. First, since the tuning parameter needs to be complexified, finding a fixed point requires the tuning of at least two real parameters. Second, the study of CCFTs has so far relied on holography [28,32], perturbative methods [14], or on the analytic continuation of real CFTs [10]. However, these methods have their limitations: for example, the range of validity of the analytic continuation is not known.

In this Letter, we propose instead to generalize the nonperturbative numerical methods which exist for 2D CFTs [33–35] to the case of complex CFTs. This enables us to provide a complete characterization of microscopic models of 2D CCFTs, including the complex central charge and scaling dimensions, the connection between scaling operators and microscopic operators, and the finite-size RG flow.

In order to demonstrate our approach, we work with the $O(n)$ loop model, which is closely related to the Q -state Potts model in 2D and has the advantage of being self-tuned to the Potts transition surface [36]. The transition

surface, residing in the parameter space of the 2D Potts model generalized to include vacancies, separates the ferromagnetic and paramagnetic phases and contains two fixed points. One of these fixed points belongs to the Potts universality class, and the other belongs to the tricritical Potts universality [36] class. The two fixed points collide and annihilate at $Q = 4$, resulting in a weakly first-order transition for $Q \gtrsim 4$ which was recently described in terms of CCFTs in Ref. [10]. Under the mapping $n = \sqrt{Q}$, a finite (respectively diverging) correlation length in the $O(n)$ loop model corresponds to a first-order (resp. second-order) transition for the Q -state Potts model.

In this context, the first-order nature of the transition in the Potts model for $Q > 4$ is related to the well-known absence of a symmetry-breaking transition in the $O(n > 2)$ model. This absence can be understood as arising from the displacement of $O(n)$ critical points into the complex plane of the $O(n)$ temperature parameter at $n = 2$ [37]. This means the $O(n)$ model actually still harbors a critical point with a diverging correlation length for $n > 2$, but for a complex value of the temperature. This critical point is described by a CCFT and should lead to a “walking” RG flow on the real axis for $n \gtrsim 2$. We note that a generalization of the CCFT analysis to the $O(n)$ model was already proposed in Refs. [10,31].

Model and CFT predictions.—Starting from a truncated high-temperature expansion of the $O(n)$ model on the honeycomb lattice, one obtains a model of nonintersecting loops on the same lattice [see Fig. 1(a)] [38,39]:

$$Z = \sum_{i \in \text{loop config}} n^{N_i} x^{l_i}, \quad (1)$$

where n of the $O(n)$ model is reinterpreted as the loop fugacity and x^{-1} is the loop tension [which corresponds to the temperature of the $O(n)$ model with $x = \beta J$]. For each loop configuration i , N_i is the number of loops, and l_i is the total length of all loops. Note that the loop model is well defined even when n is not an integer.

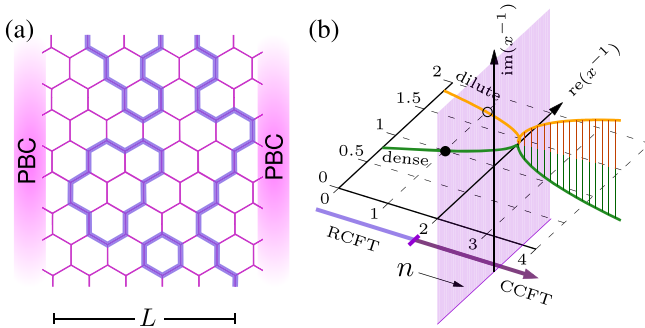


FIG. 1. (a) Example of a loop configuration on the hexagonal lattice. (b) The location of the critical branches in the complex x^{-1} plane as a function of n . The orange (resp. green) line corresponds to $x_{c,+}$ (resp. $x_{c,-}$). RCFT stands for real CFT.

This model was shown to be critical [33,34,38,40] for $-2 \leq n \leq 2$ if the loop tension sits on one of two branches:

$$x = x_{c,\pm} \equiv (2 \pm (2 - n)^{1/2})^{-1/2}. \quad (2)$$

The $x_{c,+}$ branch is the so-called dilute branch and sits at the transition between the short-loop phase in the region $x < x_{c,+}$ [which is equivalent to the high- T paramagnetic phase of the $O(n)$ model] and the critical dense loop phase in the region $x > x_{c,+}$ [see Fig. 1(b)].

Both branches have a CFT description based on Coulomb Gas [33,34,38,40–42] techniques with the following central charge:

$$c_{\pm}(n) = (4 - 7e(n)^2 \pm 3e(n)^3)/(4 - e(n)^2), \quad (3)$$

where $e(n) = (2/\pi) \cos^{-1}(n/2)$ is the background charge. A few notable examples are the Berezinskii-Kosterlitz-Thouless transition with $c_{\pm}(2) = 1$, Ising with $c_{+}(1) = 1/2$, percolation with $c_{-}(1) = 0$, and dense polymers with $c_{-}(0) = -2$.

A number of scaling dimensions are also known, like the thermal and magnetic ones [corresponding in the $O(n)$ notation to the lowest singlet and vector operator, respectively]:

$$\begin{aligned} X_{t\pm} &= 16/g_{\pm} - 2 \\ X_{h\pm} &= g_{\pm}/32 - (2/g_{\pm})(1 - g_{\pm}/4)^2 \end{aligned} \quad (4)$$

with $g_{\pm}(n) = 4 \pm 2e(n)$. The thermal scaling dimension probes the response to a change in the loop tension, or equivalently to a change in temperature of the original $O(n)$ model. The magnetic exponent describes the spin-spin correlations of the original $O(n)$ model.

In order to extend the above CFT predictions to the case of complex CFTs for $n > 2$, we follow Ref. [10], in which an analytic continuation of known CFT predictions for the $Q \leq 4$ Potts model was continued to $Q > 4$. Since the Q -state Potts model and the $O(n)$ loop models realize the same CFT branches for $Q = n^2$, it is natural to use the same analytic continuation here for the $O(n > 2)$ loop model. [Note however that the operator content is different for these two theories, and that no equivalent of Eq. (2) exists for the Potts model].

Based on Eq. (2), one finds that the two critical branches meet at $n = 2$, and move to the complex plane for $n > 2$ [see Fig. 1(b)]. Relatedly, one can easily see from Eqs. (3) and (4) that the value of the central charge and of the scaling dimensions becomes complex for $n > 2$ [see continuous lines in Figs. 2(b)–2(d)]. Note that, for $n > 2$, the two branches are simply complex conjugates of each other ($x_{c,+} = x_{c,-}^*$, $c_{+} = c_{-}^*$, and $X_{+} = X_{-}^*$), whereas for $n < 2$ they correspond to very different physics.

Numerics at the fixed points.—We now use transfer matrix numerics to verify the predictions summarized in Eqs. (2)–(4). We use periodic boundary conditions (PBCs) along the horizontal direction such that the system forms a long cylinder with a circumference of size L [see Fig. 1(a)]. Our implementation of the transfer matrix generalizes the one of Refs. [33,43] and is detailed in the Supplemental Material [44].

If we order the eigenvalues of the transfer matrix by their magnitude, $|\lambda_{L,0}| \geq |\lambda_{L,1}| \geq \dots$, the free energy per site in the long cylinder limit is given by [33–35]

$$F_L = \frac{2}{\sqrt{3}L} \log(\lambda_{L,0}). \quad (5)$$

An estimate for the central charge is then obtained by finite-size scaling through $F_L = F_\infty + (\pi c/6L^2)$.

The finite-size estimate of the thermal scaling dimension is related to the gap between $\lambda_{L,0}$ and the subleading eigenvalue $\lambda_{L,1}$:

$$X_t = \frac{2\pi}{L} \log\left(\frac{\lambda_{L,0}}{\lambda_{L,1}}\right). \quad (6)$$

In order to calculate the magnetic scaling dimension, it is necessary to define another Hilbert space sector (the so-called magnetic sector) for which there is a single non-contractible loop traversing the whole cylinder vertically. Denoting the leading eigenvalue in that sector as $\tilde{\lambda}_{L,0}$, the estimate for X_h is

$$X_h = \frac{2\pi}{L} \log\left(\frac{\lambda_{L,0}}{\tilde{\lambda}_{L,0}}\right). \quad (7)$$

The numerical results for the real and imaginary parts of c , X_t , and X_h at $x = x_{c,\pm}$ are in perfect agreement with the CFT predictions for a broad range of loop fugacities above $n = 2$. We show results up to $n = 5$ in Fig. 2, but the agreement actually persists until $n = n_g \simeq 12.34$. We have thus confirmed the existence of CCFTs in the range $n \in [2, n_g]$.

As shown in Fig. 2(e) (see also the Supplemental Material [44]), we find a level crossing at $n = n_g$ [45] beyond which the transfer matrix is gapped [i.e., $\log(|\lambda_{L,0}|/|\lambda_{L,1}|) \sim \mathcal{O}(1)$], which means the system has a finite correlation length. By inspection of the dominant eigenstate for $n > n_g$, it appears likely that the corresponding phase is adiabatically connected to the short loop phase obtained for $x \rightarrow 0$. We leave the study of the range $n > n_g$ for future work and now focus on $n \in [2, n_g]$.

RG flow and phase diagram.—Now that we have established the existence of CCFTs for $n > 2$, let us discuss their broader significance for the phase diagram and the RG flow. The standard scenario is that the presence of a complex CFT right above the real axis leads to a slowing down of the RG flow on the real axis, and hence the walking behavior.

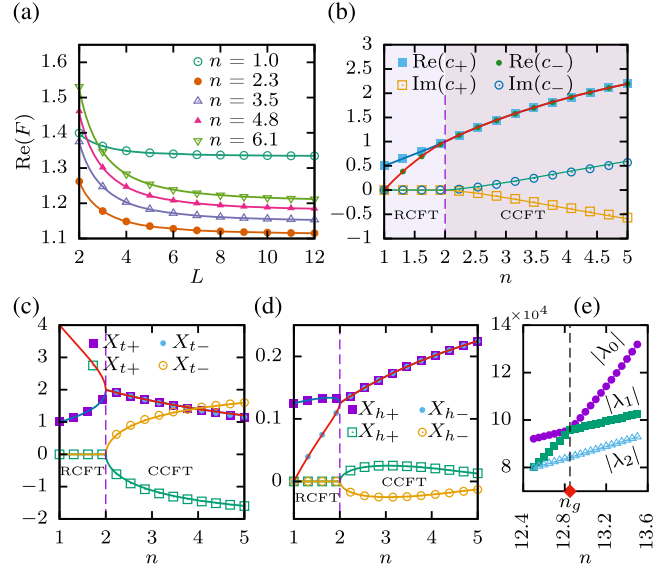


FIG. 2. (a) Real part of the free energy vs system size for various n . Solid line shows fit to $F_L = F_\infty + (\pi c/6L^2)$. The fits were calculated using numerical data points starting from $L = 4$ to $L = 12$. Real and imaginary parts of (b) the complex central charge c_\pm for the two branches, (c) the thermal scaling dimension $X_{t\pm}$, and (d) the magnetic scaling dimension $X_{h\pm}$. In (b)–(d), the solid lines are CFT predictions and the dots are numerical results. All the results are calculated at $x = x_{c,\pm}$. The scaling dimensions $X_{t\pm}$ (c) and $X_{h\pm}$ (d) are obtained for $L = 11$. (e) Magnitude of the largest three eigenvalues of the transfer matrix (for $L = 10$), showing a transition for λ_0 at $n = n_g$.

This is usually understood with the following “simple” beta function: $\beta_{\text{sim}}(x) = -\mu - (x - x_0)^2$, where $\mu < 0$ corresponds to real CFTs on the real axis, and $\mu > 0$ corresponds to complex CFTs located at $x = x_0 \pm i\sqrt{\mu}$ [see Figs. 3(a) and 3(b)].

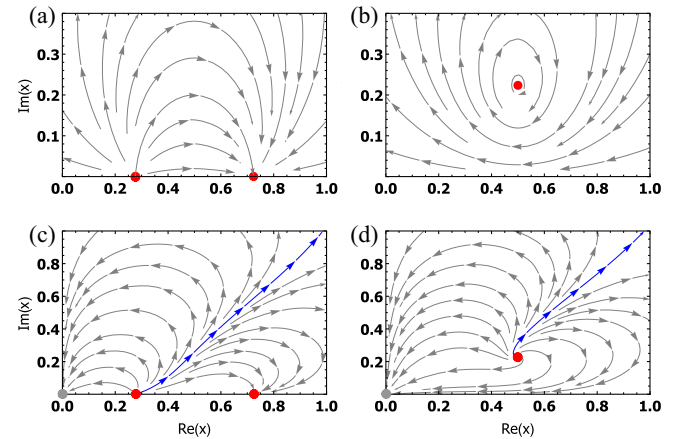


FIG. 3. Top: RG flow for the simple beta function $\beta_{\text{sim}}(x) = -\mu - (x - x_0)^2$ with $x_0 = 0.5$ and with (a) $\mu = -0.05$ or (b) $\mu = 0.05$. Bottom: RG flow for the generalized beta function $\beta_{\text{gen}}(x)$ for (c) $\mu = -0.05$ or for (d) $\mu = 0.05$. The separatrix is shown in blue. The red dots show the critical points, and the gray dot shows the gapped short loop fixed point at $x = 0$.

However, this beta function fails to capture several properties of the flow. First of all, it predicts $(d\delta x/dl) = i\sqrt{\mu}\delta x + \mathcal{O}(\delta x^2)$, with $\delta x = x - x_c$ the distance from the fixed point, which means the flow is actually circular around the CCFT until higher order terms in δx are included. This is not the case for our model since the linearized flow close to the fixed point is given by the scaling dimension $(d\delta x/dl) = (2 - X_t)\delta x + \mathcal{O}(\delta x^2)$, and $\text{Re}(2 - X_t) \neq 0$.

Second, for any n , there should be an attractive fixed point at $x = 0$ corresponding to the short loop phase [high- T phase of the $O(n)$ model]. We thus expect most of the trajectories emanating from the CCFT to reach $x = 0$. However, since the flow around the CCFT is a spiral, there needs to be a separatrix separating the trajectories which pass to the right or the left of the CCFT [see Fig. 3(d)]. These features can be reproduced with the following generalized beta function:

$$\beta_{\text{gen}}(x) = x(-\mu - (x - x_0)^2)(-\mu - (x + x_0)^2), \quad (8)$$

where we added fixed points in the left plane which should be there by $x \rightarrow -x$ symmetry since the number of loop strands is always even.

What is the origin of the separatrix shown in blue in Fig. 3? A way to study this is to look at the thermal gap X_t in the complex x plane [see Fig. 4 (top)]. We find that a line of $\text{Re}(X_t) = 0$ approaches the CCFT as $L \rightarrow \infty$. Such a line is called *equimodular* since it corresponds to $|\lambda_0| = |\lambda_1|$, and it is expected to host a finite density of zeros of the partition function in the thermodynamic limit [46]. Following earlier work [47,48], we propose to identify this line of zeros with the separatrix of the RG flow. This line should approach the fixed point as L goes to infinity following the spiral RG flow. In the Supplemental Material [44], we show a finite-size study of this flow based on the magnetic gap X_h . This scenario is reminiscent of the Lee-Yang edge singularity on the imaginary axis of the magnetic field for the Ising model at $T > T_c$. There, a line of zeros on the imaginary axis ends at a finite imaginary magnetic field ih_c with the nonunitary Lee-Yang CFT [49,50]. Note that the Lee-Yang CFT sits on the imaginary axis, and its line of zeros approaches the critical point as a straight line, whereas here the line of zeros should actually approach the CCFT following a spiral.

The equimodular line can also be understood as a first-order transition line since it corresponds to a crossing of the two dominant eigenvalues of the transfer matrix. Based on an inspection of the corresponding eigenvectors (see the Supplemental Material [44]), we interpret this first-order line as a transition between a gas phase to the left and a liquid phase to the right. Pictorially [see Fig. 4 (bottom)], the gas phase is described as a dilute gas of single-hexagon loops, whereas the liquid phase has a comparatively larger weight on longer loops. In this context, the CCFT is thus

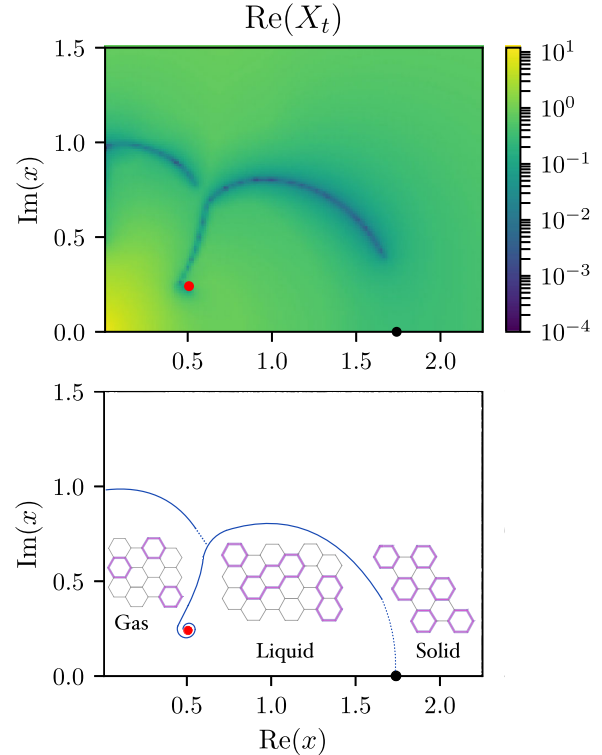


FIG. 4. Top: scaled gap $\text{Re}(X_t) \equiv (2\pi/L) \log(|\lambda_0|/|\lambda_1|)$ for $n = 8$ and $L = 9$. Note that we restricted the calculation of eigenvalues to the translation-invariant sector. The deep blue lines indicate equimodular lines. One of them approaches the predicted position of the CCFT $x_c(n)$, shown as a red dot. The black dot is the location of the $Q = 3$ Potts transition $x_p(n = 8)$ from Ref. [51]. Bottom: phase diagram suggested by the top panel. The inserts show pictorial representations of the three phases.

interpreted as a liquid-gas critical point located at the end of a first-order transition line.

Based on Fig. 3(d), we expect that all trajectories emanating from the CCFT end up at $x = 0$, except for the separatrix. However, the question remains of where the separatrix ends. Figure 4 strongly suggests that it connects to another critical point which was previously reported to emanate from the $x = \infty$ point at $n > 2$ in the $O(n)$ loop model [51]. Indeed, at large x , another bifurcation of critical points was observed at $n = 2$ in the $O(n)$ loop model: a repulsive fixed point at $x^{-1} = 0$ for $n \leq 2$ (describing so-called fully packed loops [35]) splits at $n = 2$ into a repulsive fixed point at $x = x_p(n)$ and an attractive gapped fixed point at $x^{-1} = 0$ which corresponds to a hard hexagon solid with a threefold breaking of translation invariance. The critical point at $x = x_p(n)$ was studied numerically in Ref. [51] and was found to be consistent with $Q = 3$ Potts criticality when n is sufficiently large. Overall, this suggests a gas-liquid-solid phase diagram with a liquid-gas first-order line ending in a CCFT, and a melting transition described by $Q = 3$ Potts. We note that our conjectured beta function could be verified through a numerical RG analysis [47].

Discussion.—In conclusion, we have established numerically the presence of CCFTs in the $O(n)$ loop model for $2 < n < n_g$, with $n_g \approx 12.34$. We have also proposed a phenomenological beta function which reproduces the main features of the model, including a line of zeros which approaches the CCFT as $L \rightarrow \infty$ and serves as a separatrix for the RG flow. We propose that this line of zeros can be understood as a first-order line transition between a gaslike and a liquidlike phase. We hope our results motivate further work on CCFTs in other contexts, like for non-Hermitian Hamiltonians or “strange correlators” [52–54].

Regarding the abrupt disappearance of the CCFTs at n_g , an interesting observation is that $\text{Arg}[x_{c,\pm}(n_g)] \simeq \mp \pi/6$. In the large- n limit, typical configurations are dominated by the shortest loops, which are hexagons of length 6. The fugacity of these loops is nx^6 , and the partition function thus becomes real for $\text{Arg}[x] = \pm\pi/6$, which would explain why a CCFT cannot exist at that angle of the complex x plane. This argument is however only strictly correct in the large- n limit, and its extension to finite n is left for future work.

A final point of discussion is the relation between the original $O(n)$ model and its loop formulation. The main difference between the two is that the former allows for loop crossings [55]. Loop crossings correspond to 4-leg watermelon operators with scaling dimension $X_{l=4} = 3g/8 - 2/g + 1$, which are irrelevant [i.e., $\text{Re}(X_{l=4}) > 2$] for all $n > 2$, so the CCFTs should exist in the original $O(n)$ model as well.

We would like to thank Adam Nahum for invaluable contributions to the manuscript and Xiangyu Cao for illuminating discussions. T.S. acknowledges the support of the Natural Sciences and Engineering Research Council of Canada (NSERC), in particular the Discovery Grant (No. RGPIN-2020-05842), the Accelerator Supplement (No. RGPAS-2020-00060), and the Discovery Launch Supplement (No. DGEGR-2020-00222). This research was enabled in part by support provided by Compute Canada. Research at Perimeter Institute is supported in part by the Government of Canada through the Department of Innovation, Science and Economic Development Canada and by the Province of Ontario through the Ministry of Colleges and Universities.

*These authors contributed equally to this work.

- [1] M. Nauenberg and D. J. Scalapino, Singularities and Scaling Functions at the Potts-Model Multicritical Point, *Phys. Rev. Lett.* **44**, 837 (1980).
- [2] John L. Cardy, M. Nauenberg, and D. J. Scalapino, Scaling theory of the Potts-model multicritical point, *Phys. Rev. B* **22**, 2560 (1980).
- [3] J L Cardy, General discrete planar models in two dimensions: Duality properties and phase diagrams, *J. Phys. A* **13**, 1507 (1980).
- [4] M. Fukugita and M. Okawa, Correlation Length of the Three-State Potts Model in Three Dimensions, *Phys. Rev. Lett.* **63**, 13 (1989).
- [5] Mitsuhiro Itakura, Monte Carlo renormalization group study of the Heisenberg and the XY antiferromagnet on the stacked triangular lattice and the chiral ϕ^4 model, *J. Phys. Soc. Jpn.* **72**, 74 (2003).
- [6] David B. Kaplan, Jong-Wan Lee, Dam T. Son, and Mikhail A. Stephanov, Conformality lost, *Phys. Rev. D* **80**, 125005 (2009).
- [7] Adam Nahum, J. T. Chalker, P. Serna, M. Ortuño, and A. M. Somoza, Deconfined Quantum Criticality, Scaling Violations, and Classical Loop Models, *Phys. Rev. X* **5**, 041048 (2015).
- [8] Chong Wang, Adam Nahum, Max A. Metlitski, Cenke Xu, and T. Senthil, Deconfined Quantum Critical Points: Symmetries and Dualities, *Phys. Rev. X* **7**, 031051 (2017).
- [9] Victor Gorbenko, Slava Rychkov, and Bernardo Zan, Walking, weak first-order transitions, and complex CFTs, *J. High Energy Phys.* **10** (2018) 108.
- [10] Victor Gorbenko, Slava Rychkov, and Bernardo Zan, Walking, weak first-order transitions, and complex CFTs II. Two-dimensional Potts model at $Q > 4$, *SciPost Phys.* **5**, 050 (2018).
- [11] Shumpei Iino, Satoshi Morita, Naoki Kawashima, and Anders W. Sandvik, Detecting signals of weakly first-order phase transitions in two-dimensional Potts models, *J. Phys. Soc. Jpn.* **88**, 034006 (2019).
- [12] Pablo Serna and Adam Nahum, Emergence and spontaneous breaking of approximate $O(4)$ symmetry at a weakly first-order deconfined phase transition, *Phys. Rev. B* **99**, 195110 (2019).
- [13] Han Ma and Yin-Chen He, Shadow of complex fixed point: Approximate conformality of $q > 4$ Potts model, *Phys. Rev. B* **99**, 195130 (2019).
- [14] Francesco Benini, Cristoforo Iossa, and Marco Serone, Conformality Loss, Walking, and 4D Complex Conformal Field Theories at Weak Coupling, *Phys. Rev. Lett.* **124**, 051602 (2020).
- [15] Jonathan D’Emidio, Alexander A. Eberharter, and Andreas M. Läuchli, Diagnosing weakly first-order phase transitions by coupling to order parameters, [arXiv:2106.15462](https://arxiv.org/abs/2106.15462).
- [16] Ingrid Rotter, A non-Hermitian Hamilton operator and the physics of open quantum systems, *J. Phys. A* **42**, 153001 (2009).
- [17] Frank Verstraete, Michael M. Wolf, and J. Ignacio Cirac, Quantum computation and quantum-state engineering driven by dissipation, *Nat. Phys.* **5**, 633 (2009).
- [18] Ming Lu, Xiao-Xiao Zhang, and Marcel Franz, Magnetic Suppression of Non-Hermitian Skin Effects, *Phys. Rev. Lett.* **127**, 256402 (2021).
- [19] Hilary M. Hurst and Benedetta Flebus, Perspective: Non-Hermitian physics in magnetic systems, *J. Appl. Phys.* **132**, 220902 (2022).
- [20] Emil J. Bergholtz, Jan Carl Budich, and Flore K. Kunst, Exceptional topology of non-Hermitian systems, *Rev. Mod. Phys.* **93**, 015005 (2021).
- [21] Zongping Gong, Yuto Ashida, Kohei Kawabata, Kazuaki Takasan, Sho Higashikawa, and Masahito Ueda,

- Topological Phases of Non-Hermitian Systems, *Phys. Rev. X* **8**, 031079 (2018).
- [22] Hengyun Zhou and Jong Yeon Lee, Periodic table for topological bands with non-Hermitian symmetries, *Phys. Rev. B* **99**, 235112 (2019).
- [23] Zongping Gong, Yuto Ashida, Kohei Kawabata, Kazuaki Takasan, Sho Higashikawa, and Masahito Ueda, Topological Phases of Non-Hermitian Systems, *Phys. Rev. X* **8**, 031079 (2018).
- [24] Norifumi Matsumoto, Kohei Kawabata, Yuto Ashida, Shunsuke Furukawa, and Masahito Ueda, Continuous Phase Transition without Gap Closing in Non-Hermitian Quantum Many-Body Systems, *Phys. Rev. Lett.* **125**, 260601 (2020).
- [25] Chang-Tse Hsieh and Po-Yao Chang, Relating non-Hermitian and Hermitian quantum systems at criticality, [arXiv:2211.12525](https://arxiv.org/abs/2211.12525).
- [26] C. Itzykson, H. Saleur, and J. B. Zuber, Conformal invariance of nonunitary 2D-models, *Europhys. Lett.* **2**, 91 (1986).
- [27] John L. Cardy, Conformal Invariance and the Yang-Lee Edge Singularity in Two Dimensions, *Phys. Rev. Lett.* **54**, 1354 (1985).
- [28] Antón F. Faedo, Carlos Hoyos, David Mateos, and Javier G. Subils, Holographic Complex Conformal Field Theories, *Phys. Rev. Lett.* **124**, 161601 (2020).
- [29] Simone Giombi, Richard Huang, Igor R. Klebanov, Silviu S. Pufu, and Grigory Tarnopolsky, The $O(N)$ model in $4 < d < 6$: Instantons and complex CFTs, *Phys. Rev. D* **101**, 045013 (2020).
- [30] Dario Benedetti, Instability of complex CFTs with operators in the principal series, *J. High Energy Phys.* **05** (2021) 004.
- [31] Victor Gorbenko and Bernardo Zan, Two-dimensional $O(n)$ models and logarithmic CFTs, *J. High Energy Phys.* **10** (2020) 099.
- [32] Antón F. Faedo, Carlos Hoyos, David Mateos, and Javier G. Subils, Multiple mass hierarchies from complex fixed point collisions, *J. High Energy Phys.* **10** (2021) 246.
- [33] H. W. J. Blöte and B. Nienhuis, Critical behaviour and conformal anomaly of the $O(n)$ model on the square lattice, *J. Phys. A* **22**, 1415 (1989).
- [34] Murray T. Batchelor and Henk W. J. Blöte, Conformal Anomaly and Scaling Dimensions of the $O(n)$ Model from an Exact Solution on the Honeycomb Lattice, *Phys. Rev. Lett.* **61**, 138 (1988).
- [35] H. W. J. Blöte and B. Nienhuis, Fully Packed Loop Model on the Honeycomb Lattice, *Phys. Rev. Lett.* **72**, 1372 (1994).
- [36] Bernard Nienhuis, Locus of the tricritical transition in a two-dimensional Q-state Potts model, *Physica (Amsterdam)* **177A**, 109 (1991).
- [37] Note that the temperature of the $O(n)$ model does not map to the temperature of the Potts model.
- [38] Bernard Nienhuis, Exact Critical Point and Critical Exponents of $O(n)$ Models in Two Dimensions, *Phys. Rev. Lett.* **49**, 1062 (1982).
- [39] Ron Peled and Yinon Spinka, Lectures on the spin and loop $O(n)$ models, [arXiv:1708.00058](https://arxiv.org/abs/1708.00058).
- [40] R. J. Baxter, Q colourings of the triangular lattice, *J. Phys. A* **19**, 2821 (1986).
- [41] P. di Francesco, H. Saleur, and J. B. Zuber, Relations between the Coulomb gas picture and conformal invariance of two-dimensional critical models, *J. Stat. Phys.* **49**, 57 (1987).
- [42] Jesper Lykke Jacobsen, Conformal field theory applied to loop models, in *Polygons, Polyominoes and Polycubes*, edited by Anthony J. Guttmann (Springer Netherlands, Dordrecht, 2009), pp. 347–424.
- [43] Henk W. J. Blöte and Bernard Nienhuis, The phase diagram of the $O(n)$ model, *Physica (Amsterdam)* **160A**, 121 (1989).
- [44] See Supplemental Material at <http://link.aps.org/supplemental/10.1103/PhysRevLett.131.131601> for more details on the numerical determination of n_g , an analysis of the magnetic gap, a description of the transfer matrix calculations, and a characterization of the gas and liquid phases.
- [45] Note that the two eigenvalues only cross in magnitude but not in phase.
- [46] M. Assis, J. L. Jacobsen, I. Jensen, J.-M. Maillard, and B. M. McCoy, The hard hexagon partition function for complex fugacity, *J. Phys. A* **46**, 445202 (2013), Appendix F.
- [47] Yuzhi Liu and Y. Meurice, Lines of Fisher's zeros as separatrices for complex renormalization group flows, *Phys. Rev. D* **83**, 096008 (2011).
- [48] Seung-Yeon Kim, Chi-Ok Hwang, and Jin Min Kim, Partition function zeros of the antiferromagnetic Ising model on triangular lattice in the complex temperature plane for nonzero magnetic field, *Nucl. Phys.* **B805**, 441 (2008).
- [49] Michael E. Fisher and Yang-Lee, Edge Singularity and ϕ^3 Field Theory, *Phys. Rev. Lett.* **40**, 1610 (1978).
- [50] John L. Cardy, Conformal Invariance and the Yang-Lee Edge Singularity in Two Dimensions, *Phys. Rev. Lett.* **54**, 1354 (1985).
- [51] Wenan Guo, Henk W. J. Blöte, and F. Y. Wu, Phase Transition in the $n > 2$ Honeycomb $O(n)$ Model, *Phys. Rev. Lett.* **85**, 3874 (2000).
- [52] Yi-Zhuang You, Zhen Bi, Alex Rasmussen, Kevin Slagle, and Cenke Xu, Wave Function and Strange Correlator of Short-Range Entangled States, *Phys. Rev. Lett.* **112**, 247202 (2014).
- [53] Thomas Scaffidi and Zohar Ringel, Wave functions of symmetry-protected topological phases from conformal field theories, *Phys. Rev. B* **93**, 115105 (2016).
- [54] Thomas Scaffidi, Daniel E. Parker, and Romain Vasseur, Gapless Symmetry-Protected Topological Order, *Phys. Rev. X* **7**, 041048 (2017).
- [55] J. L. Jacobsen, N. Read, and H. Saleur, Dense Loops, Supersymmetry, and Goldstone Phases in Two Dimensions, *Phys. Rev. Lett.* **90**, 090601 (2003).